Damage Detection of CNT/CNC-reinforced Foam-cored Sandwich Composites by Acoustic Emission Tests under Flexural Load

Kucukkalfa, Eyuphan ; Ghaderiaram, A.; Yildiz , Kaan; Fotouhi, M.; Asadi, Amir ; Cebeci, Hulya

DOI
10.2514/6.2023-2030

Publication date
2023

Document Version
Final published version

Published in
AIAA SciTech Forum 2023

AIAA SciTech Forum
23-27 January 2023, National Harbor, MD & Online
AIAA SCITECH 2023 Forum

10.2514/6.2023-2030

Damage Detection of CNT/CNC-reinforced Foam-cored Sandwich Composites by Acoustic Emission Tests under Flexural Load

Eyuphan Kucukkalfa[1] and Kaan Yildiz[3]
Aviation Institute, Istanbul Technical University, Istanbul 34467, Turkey
Aerospace Research Center, Istanbul Technical University, Istanbul 34467, Turkey

Aliakbar Ghaderiaram[2] and Mohammad Fotouhi [4]
MICROLAB, Faculty of Civil Engineering and Geosciences, Delft University of Technology, Delft, 2628 CN, the Netherlands

Amir Asadi[5]
Department of Engineering Technology & Industrial Distribution, Texas A&M University, College Station, TX 77843-336, USA

Hulya Cebeci[6]
Faculty of Aeronautics and Astronautics, Istanbul Technical University, Istanbul 34467, Turkey
Aerospace Research Center, Istanbul Technical University, Istanbul 34467, Turkey

Sandwich composites stand out especially in the aerospace industry owing to their high strength-to-weight ratio, one of the most prominent factors for material selection. Polymeric foams as core material in sandwich composites are likely to prevent delamination between face sheets and core by augmenting the contact surface area, resulting from their closed-cell structure. Polymeric foam properties can be enhanced by adding nanomaterials such as carbon nanotubes (CNTs), however increased CNT content or the type of CNTs might arise critical problems such as agglomeration and irregular distribution of nanomaterials. Cellulose nanocrystals (CNCs) are claimed to be good candidates to prevent nanomaterial reinforcing related issues and further, their inclusion enables reinforcing of polymeric foams using an optimum CNT/CNC concentration. In this work, CNT/CNC reinforced polyurethane (PU) foam-cored sandwich composites were manufactured and characterized for the influence of nanomaterial addition on the mechanical properties with an aim to find the optimum nanomaterial content. 0.1 wt.% CNT, CNC, CNT/CNC (1:1), and CNT/CNC (1:2) reinforced PU foam-cored sandwich composites were subjected to simultaneous three-point bending tests and acoustic emission tests, one of the promising non-destructive testing methods enabling in-situ monitoring of the damage mechanisms to understand how damage evolves. The effects of these nanomaterial additives on damage mechanisms and the mechanical properties were

[1] Research Assistant, Aviation Institute.
[2] PhD Researcher, Civil Engineering and Geosciences.
[3] Assistant Professor, Aviation Institute.
[4] Assistant Professor, Civil Engineering and Geosciences.
[5] Assistant Professor, Engineering Technology & Industrial Distribution.
[6] Associate Professor, Department of Aeronautical Engineering, AIAA Member.

examined thoroughly via both mechanical and morphological characterizations. The test results were found to be promising in terms of revealing how these reinforcements affect the retardation and/or elimination of damage mechanisms including core damage, face sheet-core debonding, matrix cracking, and fiber breakage in the sandwich composite structures. The results suggested that with the addition of 0.1 wt.% CNT, the mechanical properties of PU foam were increased; therefore, the ratio of AE signals related to fiber breakage and core damage were decreased because of the strengthened core material.

I. Nomenclature

σ_c	=	compressive stress
ε_c	=	compressive strain
σ_f	=	flexural stress
ε_f	=	flexural strain
P	=	applied load
A	=	cross-section area
h	=	stroke height
h_0	=	initial specimen height
D	=	maximum deflection at the center of the beam
d	=	depth of the beam
L	=	support span
b	=	width of the beam
N	=	cell density
n	=	number of cells
M	=	magnification factor
A	=	micrograph area

II. Introduction

Polymeric foams, with a closed-cell structure that increases the contact surface area between face sheets and cores of sandwich composites, are an excellent alternative to honeycomb cores, which have an open-cell structure and are prone to debonding between face sheets and cores. Besides their high strength-to-weight ratio, impact resistance, and sound absorption capabilities, polymeric foams can be functionalized and strengthened by reinforcing with nanomaterials such as carbon nanotube (CNT) [1, 2], carbon nanofiber (CNF) [3], nano clay [4], titanium dioxide (TiO_2) [4], aluminum oxide [5], cellulose nanocrystal (CNC) [6], and glass fiber [7-9]. Ciecierska et al. [1] reinforced polyurethane (PU) foams with CNTs up to 0.05 wt.% where 21% increase in bending strength was shown to be viable. In addition, Navidfar et al. [2] reinforced PU foams with CNTs up to 0.25 wt.% obtaining 15% increase in tensile strength. Furthermore, Mafhuz et al. [3] used CNF as a reinforcement in PU foam-cored sandwich composites and achieved 19% and 33% increases in shear modulus and strength, respectively. In a study by Saha et al. [4], TiO_2 and nano clay reinforcement of PU foams were examined, with nano clay providing 69.3% enhancement in tensile modulus and TiO_2 providing 12.4% increase in compressive modulus. Whereas, Septevani et al. [6] attained 16.74% enhancement in compressive modulus by CNC reinforcement, Şerban et al. [7] and Yu et al. [8] reached 68.9% and 35% increases in tensile modulus and compressive strength, respectively, by glass fiber reinforcement of PU foam, respectively.

Because of their high strength and light weight, CNTs are frequently used as a reinforcing material. However, when the amount of CNT reinforcement is relatively high, challenges such as agglomeration and non-uniform dispersion/distribution appear in the foam structure, producing materials with inferior mechanical properties [10]. As a result, integrating auxiliary nanomaterials, e.g., CNCs, can prevent CNTs from establishing strong Van der Waals bonds among themselves, enabling a more uniform dispersion in the foam structure. For the effective dispersion of CNTs and CNCs, distilled water is proposed to be one of the most accessible and appropriate liquids. Considering the chemical structure of CNCs, they provide colloidal stability by bonding with distilled water thanks to their hydrophilic parts and their bonding ability with CNTs through nonpolar parts [11]. After vaporizing distilled water, polymeric foams could be reinforced with the optimum CNT/CNC powder concentration.

Despite the aforementioned potential of replacing honeycomb, foam-filled sandwich composites also suffer from same type of damage mechanisms. In a study by Assarar et al. [12], it was mentioned that foam-cored sandwich composites have various damage mechanisms such as core damage, matrix cracking, face sheet-core debonding, fiber

matrix separation, and fiber breakage under load. When it comes to identify the damage mechanisms, the non-destructive testing method, *acoustic emission (AE) test* can be used to analyze the type of failure for structural health monitoring of materials [13, 14], to prevent any potential irreversible damage and to strengthen materials. Several clustering methods such as wavelet packet transform (WPT), fuzzy clustering method (FCM) and k-means genetic algorithm can be utilized in conjunction with a principal component analysis (PCA) to distinguish AE signals caused by various types of damage mechanisms [15]. The amplitude data of the captured AE signals was used in several studies [12, 14, 16] to determine the failure mechanisms of foam-cored sandwich composites. However, it was seen from these studies that solely the amplitude data was not sufficient to distinguish damage mechanisms rationally. Therefore, to alleviate this ambiguity, several authors suggested the use of peak frequency and cumulative energy data for well-distinguished damage detection [17-19]. For instance, Pashmforoush et al. [19] stated that the k-means genetic algorithm is one of the most suitable clustering algorithms for damage classification using the peak frequency and the cumulative energy data.

In this work, acoustic emission tests were conducted simultaneously with the three-point bending tests to mechanically characterize the PU foam-cored sandwich composites reinforced with 0.1 wt.% CNT, CNC, and CNT/CNC with the ratios of 1:1 (0.05 wt.% CNT and 0.05 wt.% CNC) and 1:2 (0.033 wt.% CNT and 0.066 wt.% CNC). The reinforcement ratio of neat PU foam was decided as 0.1 wt.% based on our previous studies [20, 21] where same materials were utilized and reasonable enhancements were attained. The influence of these nanomaterial reinforcements on the failure mechanisms, damage modes and mechanical properties were analyzed to determine an optimum CNT/CNC content to enhance the mechanical properties while not causing additional issues on the morphology of the foams. Moreover, SEM images were utilized to investigate the influence of nano material reinforcement on the microstructure-material property relation of PU foams.

III. Experimental

Polyol 9022/100 and PMDI (polymeric diphenylmethane diisocyanate) for the foaming process were purchased from Active Foam, Istanbul. Multi-walled CNTs with 8-10 nm diameter and 92% purity were acquired from Nanografi, Istanbul. CNCs with 2.3-4.5 nm diameter and 44-108 nm length were purchased from Celluforce, Canada. 4 plies unidirectional carbon fiber prepregs (0/90/0/90) were used as face sheets of sandwich composites.

Initially, CNCs were sonicated for 8 minutes in distilled water using a microtip sonicator at 20% amplitude and 10 Watts. Afterwards, CNTs were added to the distilled water/CNC dispersion and the same sonication procedure were applied with ice cube treatment around the beaker to avoid overheating. Then, distilled water/CNT/CNC dispersion was poured into a petri dish and dried in an oven for 6 hours at 80 °C under 250 mbar. Finally, dried CNT/CNC were taken from the petri dish and grounded to the powder using a pestle and mortar. CNT/CNC dispersion procedure is illustrated in Fig. 1.

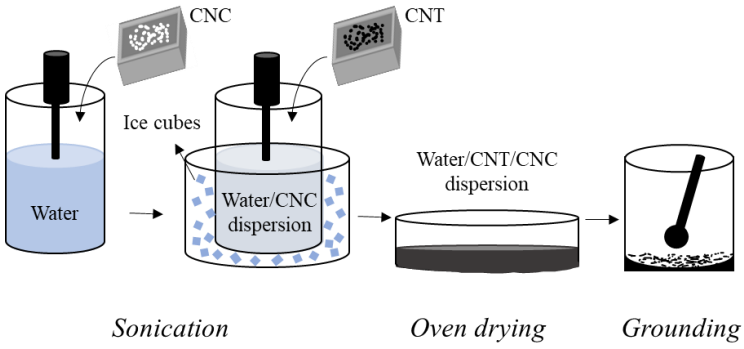

Fig. 1 CNT/CNC dispersion procedure including sonication, oven drying and grounding processes.

Nanomaterials in powder form were added to polymeric diphenylmethane diisocyanate (PMDI) part and mixed by a homogenizator for 7.5 minutes at 10000 rpm. After that, PMDI/nanomaterial were sonicated for 7.5 minutes using a horn sonicator at 30% amplitude and 40 Watts. Then, PMDI/nanomaterial and polyol were mixed with 50:50 weight ratio for 40 seconds at 2100 rpm and poured into a mold to allow free-rise of the foam for 10 minutes at room temperature. Finally, the foam was held in a 40 °C oven for 10 hours for curing. Foaming of neat and CNT/CNC reinforced PU foams is depicted in Fig. 2.

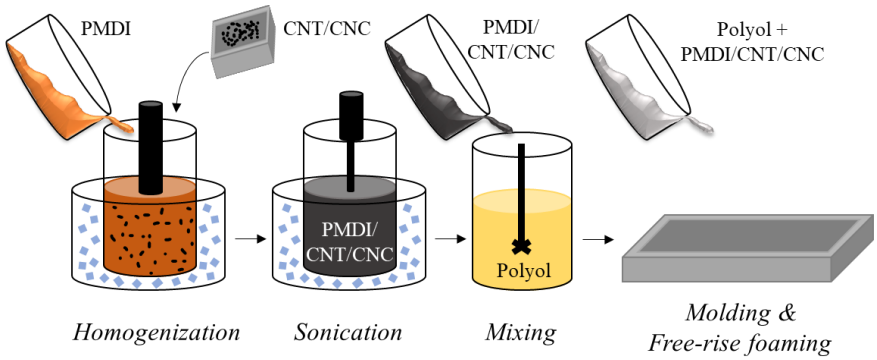

Fig. 2 Foaming of neat and CNT/CNC reinforced PU foams including homogenization, sonication, mixing and molding procedures.

Scanning electron microscopy (SEM) were utilized to examine the cellular properties of neat and nano-reinforced PU foams. SEM images were acquired under high vacuum and an accelerating voltage of 15 kV, by coating samples with a thin layer of gold prior to imaging process. The microstructure-material property relation of PU foams was evaluated by measuring and analyzing the lengths of cell edges (l), cell wall thicknesses (t), and cell densities (N) of neat and nano-reinforced foams.

Compression tests of PU foams were performed by a Shimadzu universal test machine (UTM) using a 50 kN load cell under displacement control according to ASTM C365-16 standards. Test specimens were cut to 30x30x15 mm^3 and at least 5 specimens were tested with 0.5 mm/min test speed.

Three-point bending tests were performed on displacement control using a crosshead speed of 2 mm/min on a universal computer-controlled Instron 8872 test machine with a maximum of 10kN load cell capacity related to ASTM C393 standards. The core material was cut to 150x50x15 mm^3 and 3 sandwich composite test specimens of each type were tested. Two AE sensors were located at a distance of 100 mm apart on both sides of the specimen, to monitor the damage events. An AE data acquisition system (PAC) PCI-2 with a maximum sampling rate of 40 MHz was used to record the AE signals. PAC broadband, single-crystal piezoelectric transducers were used as AE sensors. The frequency range of the sensors was 100–1000 kHz, and the gain selector of the preamplifier and the threshold value were set to 40dB. The surface of the sensor was covered with silicon grease to provide good acoustic coupling between the specimen and the sensor. The test sampling rate was 5 MHz. A pencil lead break procedure was used to calibrate the data acquisition system for each of the specimens. After the calibration step, the AE signals were recorded during the three-point bending tests as illustrated in Fig. 3.

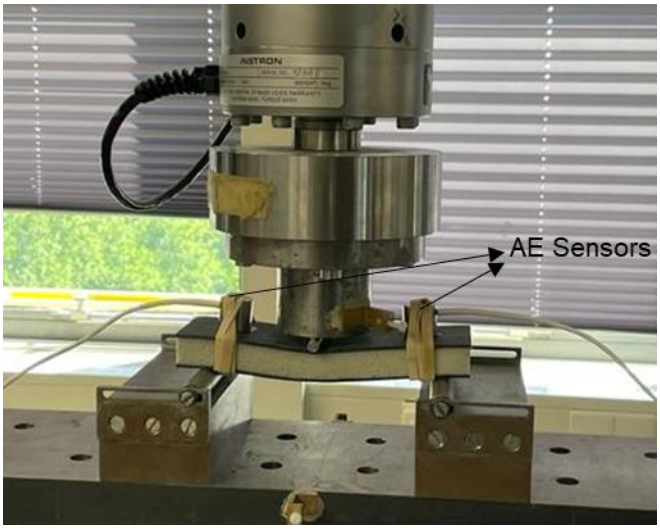

Fig. 3 Simultaneous three-point bending and acoustic emission tests of the sandwich composites using two AE sensors.

IV. Results & Discussion

In this section, SEM images were analyzed and the results were discussed in terms of the change in microstructure/mechanical properties of neat PU foams with nanomaterial reinforcement. Subsequently compression test results and three-point bending test results accompanied by AE data were presented and comprehensively discussed. Analysis of the AE data in correspondence with the three-point bending results enabled the identification of damage mechanisms in PU foam-cored sandwich composite test specimens. The results were interpreted and how the damage mechanisms are affected by the nanomaterial reinforcements was discussed. Additionally, test specimens of neat, 0.1 wt.% CNT, CNC, CNT/CNC (1:1), and CNT/CNC (1:2) reinforced PU foams were labeled as N-PU, 0.1CNT-PU, 0.1CNC-PU, 0.1CNT/CNC(1:1)-PU, and 0.1CNT/CNC(1:2)-PU, respectively.

Sections from SEM images at 200x magnification factor of the neat and nano-reinforced PU foams are shown in Fig. 4.a and Fig. 4.b, respectively. The resulting images clearly display a regular distribution among foam cells. Cell wall thickness/edge length ratio and cell density were essential to determine the increase in mechanical properties such as strength and elastic modulus. Therefore, Fig. 4 was analyzed using the ImageJ program, cell edge length (l) and cell wall thickness (t) values were measured, and Eq 1. [4] was used to calculate the cell density (N). It was observed that the cell sizes were slightly different from each other which is attributed to the heterogeneous nucleation mechanism of PU foams [20]. SEM results and morphological properties of PU foams were summarized in Table 1. As a result of the analysis and calculations, the cell edge length, cell wall thickness, wall thickness/edge length ratio, and the cell density of N-PU was found as 103.98±8.47 μm, 29.21±4.71 μm, 0.28, and 2.65×10^4 cells/cm^3, respectively. Cell edge length and cell wall thickness were decreased with each nanomaterial reinforcement type. While both t/l ratio and cell densities were increased with 0.1% wt. CNT and 0.1% wt. CNC reinforcement, t/l ratio did not change considerably for 0.1% wt. CNT/CNC(1:1)-PU and 0.1% wt. CNT/CNC(1:2)-PU.

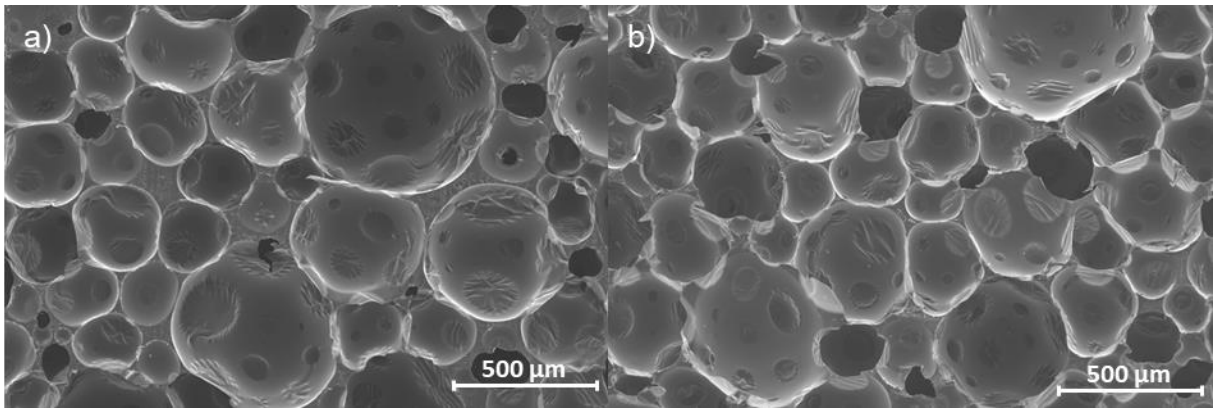

Fig. 4 Representative SEM images of a) neat and b) nano-reinforced PU foams at 200x magnification.

$$N = \left(\frac{nM^2}{A}\right)^{1.5} \tag{1}$$

Table 1 Summary of morphological properties of PU foams.

Specimen	Cell Edge Length (l) (μm)	Cell Wall Thickness (t) (μm)	t/l	Cell Density ($x10^4$ cell/cm^3)
N-PU	103.98±8.47	29.21±4.71	0.28	2.65
0.1CNT-PU	74.02±11.33	26.34±4.53	0.36	4.17
0.1CNC-PU	77.44±9.82	25.47±4.38	0.33	3.07
0.1CNT/CNC(1:1)-PU	86.79±11.25	23.32±4.00	0.27	3.43
0.1CNT/CNC(1:2)-PU	83.63±13.17	23.98±4.47	0.29	3.16

The compression tests results acquired in the form of load and displacement were converted into stress and strain data via Eq. (2) and Eq. (3). The test fixture and stress-strain data of the compression test results of PU foams are shown in Fig. 5.a. Specific compressive strength and the compressive modulus of the neat PU foam were calculated as 0.00886 MPa.m^3/kg and 29.36 MPa, respectively. The compression test results suggested that regardless of the nanomaterial concentration, no remarkable change was observed in terms of compressive strength. Nevertheless, with the addition of 0.1 wt.% CNT and 0.1 wt.% CNC, compressive moduli of the PU foams were boosted by 13.89% and 7.19%, respectively. However, on the contrary, 0.1 wt.% CNT/CNC (1:1) and 0.1 wt.% CNT/CNC (1:2) nanomaterial addition led to a decrease in the compressive moduli of PU by 15.21% and 2.87%, respectively. The underlying reasons of this behavior can be considered as the agglomerations between nanoparticles and the possibly overlooked issues during the drying process of CNT/CNC dispersion.

$$\sigma_C = P/A \tag{2}$$

$$\epsilon_C = h/h_0 \tag{3}$$

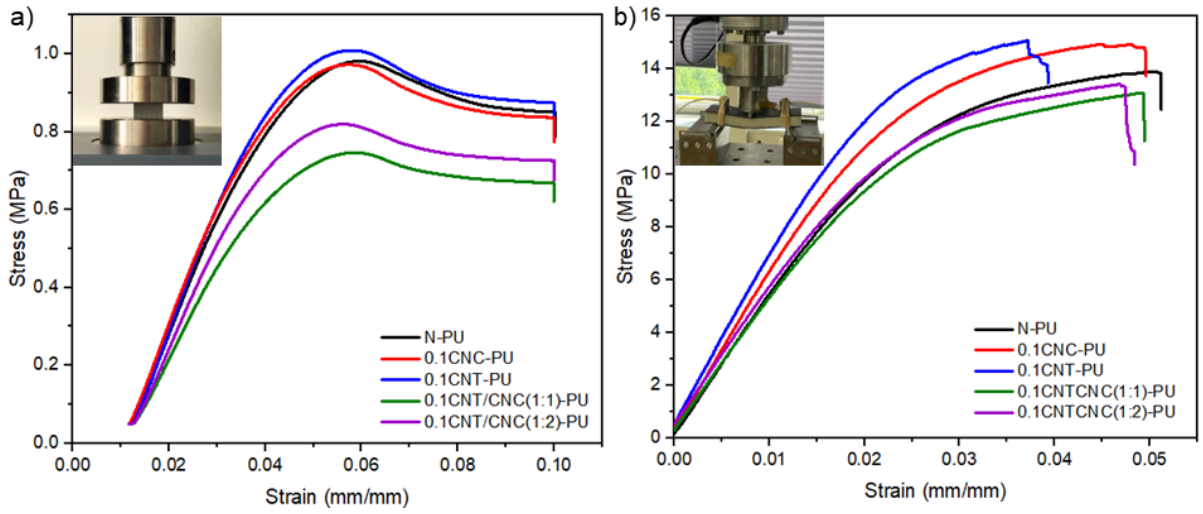

Fig. 5 Test fixture and stress-strain data of a) compression and b) three-point bending tests of PU foams.

Similarly, stress-strain data (obtained by Eq. (4) and Eq. (5)) of three-point bending test results are presented in Fig. 5.b. Flexural properties were found to be largely parallel to the results of the compression properties. Flexural performance properties of load bearing capacity, flexural strength and flexural modulus were increased by 6.84%, 6.88%, and 16.03%, respectively, for 0.1 wt.% CNT reinforced PU foam-cored sandwich composites. In addition, 7.55%, 7.07% and 14.15% enhancement in load bearing capacity, flexural strength and flexural modulus were obtained for 0.1 wt.% CNC reinforcement of the core material. Flexural properties of 1CNT-PU, 1CNT/CNC(1:1)-PU, and 1CNT/CNC(1:2)-PU did not increase due to poor dispersion quality, as a result of the agglomerations and high viscosity of PMDI/CNT blend. The reasons behind the poor mechanical properties of the specimens reinforced by CNT/CNC as low as 0.1 wt.% were considered to be drying method of the CNT/CNC aqueous dispersion. The oven drying method utilized in this study is envisaged to yield not evenly sized nanoparticles after the evaporation of the distilled water for their integration into PU foams, in return causing inferior mechanical properties. Even though individual 0.1 wt.% CNT and CNC reinforcements contributed to the mechanical properties positively, unfortunately, their combination was far from fulfilling the expectations. With the hybrid reinforcement of CNT and CNC benefiting from the CNCs bonding abilities with CNTs to prevent strong van der Waals bonds between CNTs yielded decreased mechanical properties in 0.1CNT/CNC(1:1)-PU and 0.1CNT/CNC(1:2)-PU samples. Therefore, the decline in the mechanical properties is mostly attributed to the oven drying of CNT/CNC aqueous dispersion.

$$\epsilon_f = 6Dd/L^2 \tag{4}$$

$$\sigma_f = 3PL/(2bd^2) \tag{5}$$

The collection of AE data during the three-point bending test allows clustering and identification of individual data points to determine the type of damage they correspond to. The most prominent parameters used to analyze the AE data are amplitude, peak frequency, energy, duration of the signal, and the rise time as widely noted in the

literature. However, as a typical behavior, signals belonging to different damage types might have similar amplitude and energy levels and therefore overlapping regions, making it challenging to categorize the signals. To address this problem, previous studies [17-19] revealed that the peak frequency data is a good choice for clustering and results in more accurate classification of damage mechanisms. Additionally, the decision of which cluster corresponds to which damage mechanism is greatly influenced by the cumulative energy data. Therefore, peak frequency, amplitude, energy, cumulative energy, and the number of hits were utilized to analyze the AE characteristics of the specimens. Peak frequency vs. amplitude (Fig. 6.a), load-energy vs. displacement (Fig. 6.b), and load-cumulative energy vs. displacement (Fig. 6.c) graphs were plotted for each test specimen. Following that, k-means genetic algorithm was employed to increase the effectiveness and the reliability of the damage classification, creating four clusters analogous to previous studies conducted on sandwich composites [14, 17, 19, 23, 24]. Each of these four clusters specifies a damage type which are core damage, core-face sheet debonding, matrix cracking, and fiber breakage. While core damage includes both PU foams and reinforcement materials, matrix cracking and fiber breakage represents the failures of epoxy resin and carbon fibers in laminated face sheets.

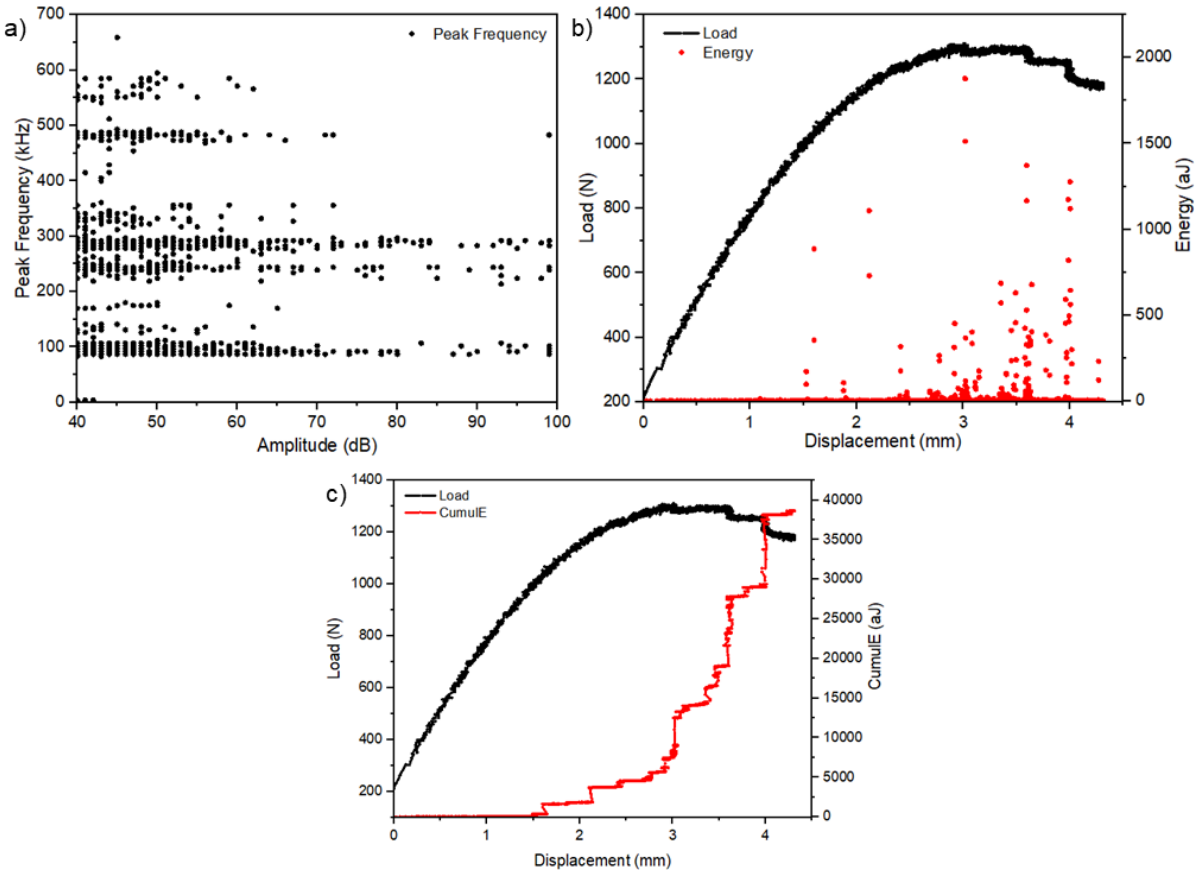

Fig. 6 Representative graphs of a) peak frequency vs. amplitude and b) load-energy vs. displacement, and c) load-cumulative energy vs. displacement, and d) load-cumulative energy vs. displacement including separate damage modes.

Fig. 7 illustrates that the AE signal clustering can be achieved considering the related peak frequency and the amplitude data. Peak frequency/amplitude data were exhibited only for N-PU,0.1CNT-PU, and 0.1CNC-PU in Fig. 7.a, Fig. 7b, and Fig. 7.c respectively; since the increase of bending properties brought on by the nanomaterial reinforcement. However, the AE data of 0.1CNT/CNC(1:1)-PU and 0.1CNT/CNC(1:1)-PU were also utilized to classify damage modes and ascertain the dominance of AE hits. It is clear that the amplitude range is not solely sufficient to separate AE data into clusters; however, when used together with the peak frequency, clusters can be distinguished easily. Thus, AE clusters were classified using peak frequency-amplitude data and indicated by different colors, i.e. blue, green, purple, and red. Moreover, considering Fig. 7 and the energy release of related AE hits using load-energy vs. displacement and load-cumulative energy vs. displacement curves, damage types were classified and presented in Table 2, from a lower frequency to a higher frequency as fiber breakage, matrix cracking, face sheet-core

debonding, and core damage. Generally, fiber breakage in face sheets of sandwich composites and laminated composites corresponds to AE data having high-frequency values in the literature [14, 15, 17, 19, 23]; whereas, some other studies claim the opposite [24, 25]. While several factors might affect the difference between the frequency outputs of the studies, specimen type (such as laminated composites and sandwich composites) and testing (i.e. tensile, double cantilever beam, and three-point bending) might be the main reasons. In this study, the AE test was applied to the foam-cored sandwich composites under simultaneous three-point bending test. Since this content has not been examined in previous studies, it is thought that the AE test results and frequency ranges are unique for this test setup. Figure 7.d illustrates that the load vs. displacement curve including cumulative energy of individual damage types. The AE data captured at the final failure during the three-point bending tests were considered as fiber breakage hits because they have both low frequency and high energy release. Likewise, the damages indicating matrix cracking were determined using the AE hits cause relatively lower cumulative energy than fiber breakage towards the final failure. In addition, AE hits having high-frequency and low-energy occurring in the first stages of the three-point bending test were determined as core damage. Accordingly, AE data with lower frequency but higher energy release than the core damage occurring at the beginning of elastoplastic stage of the three-point bending test were determined as core/face sheet debonding. Moreover, Fig. 7 illustrates that the number of AE hits are more concentrated for debonding in both 0.1CNT-PU (Fig. 7.b) and 0.1CNC-PU (Fig. 7.c) than N-PU (Fig. 7.a). Furthermore, AE data belong to core damage for 0.1CNT-PU and matrix cracking data for 0.1CNC-PU were cumulated in a narrow frequency range.

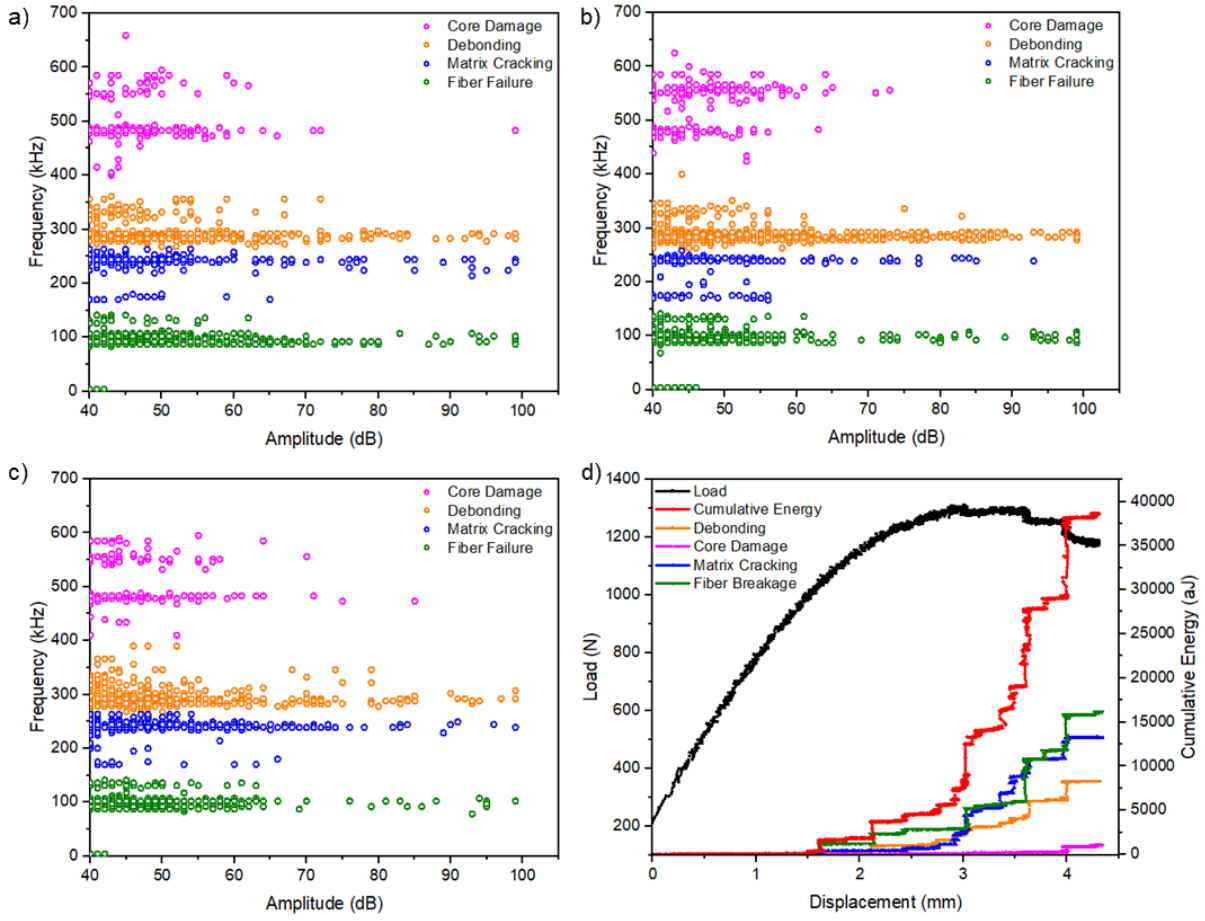

Fig. 7 Peak frequency/Amplitude data of a) N-PU, b) 0.1CNT-PU, c) 0.1CNC-PU.

Table 2: Damage types and the corresponding frequency ranges used for classification

Damage Type	Frequency Range (kHz)
Core Damage	400-750
Debonding	270-400
Matrix Cracking	170-270
Fiber Breakage	0-170

The dominance of failure mechanisms can be evaluated considering the amount and energy of AE hits. Table 3 and Table 4, illustrates the ratio of AE hits count until failure and the cumulative energy for each damage mechanism, respectively. Table 3 shows that the reinforced sandwich composites, except for 0.1 wt.% CNT and 0.1 wt.% CNC, have higher fiber breakage ratio due to earlier failure of the sandwich material which has weaken core material. Strengthened core materials with 0.1 wt.% CNT and 0.1 wt.% CNC reinforcement increase the loading resistance between face sheets and decrease the overall fiber breakage ratio. Moreover, Table 4 reveals that cumulative energy values associated with core damage and fiber breakage were reduced by six-fold and almost two-fold respectively, with 0.1 wt.% CNT reinforcement of PU foam. These results show that the best nanomaterial concentration to strengthen the core material and support the face sheets under flexural loads is found to be 0.1 wt.% CNT.

Table 3 The dominance of the number of AE hits for each damage mechanism.

Damage Type	N-PU	0.1CNT-PU	0.1CNC-PU	0.1CNT/CNC(1:1)-PU	0.1CNT/CNC(1:2)-PU
Core Damage (%)	7.37	6.64	10.76	9.99	7.08
Debonding (%)	25.82	32.82	25.93	14.06	23.14
Matrix Cracking (%)	25.25	24.68	25.77	17.38	21.59
Fiber Breakage (%)	41.56	35.86	37.54	58.57	48.19

Table 4 The dominance of cumulative energy of the AE hits for each damage mechanism.

Damage Type	N-PU	0.1CNT-PU	0.1CNC-PU	0.1CNT/CNC(1:1)-PU	0.1CNT/CNC(1:2)-PU
Core Damage (%)	3.05	0.51	1.28	3.97	0.78
Debonding (%)	11.74	43.61	22.26	17.73	28.30
Matrix Cracking (%)	20.85	18.22	27.27	10.78	11.20
Fiber Breakage (%)	64.36	37.66	49.19	67.52	59.72

V. Conclusion

In this study, PU foam cores were reinforced with 0.1 wt.% CNT, CNC, CNT/CNC (1:1), and CNT/CNC (1:2). The main objective of the study was to strengthen the PU foam core with an increased CNT content while preventing agglomerations by introducing CNC as a secondary nanomaterial reinforcement considering their chemical compatibility and dispersibility in the water together. The fabricated foam-cored sandwich composites were subjected to simultaneous three-point bending and AE tests to find out how the mechanical properties and the damage mechanisms are affected. Whereas, 0.1 wt.% CNT and CNC reinforcement of the core yielded increased mechanical properties, 0.1 wt.% CNT reinforcement exhibited the best results in terms of both compression and flexural response. Moreover, SEM images also indicated that the increases in both cell edge length/wall thickness ratio and cell density by nano reinforcement of 0.1% wt. CNT and 0.1% wt. CNC justify the enhancements in compressive and bending properties. Furthermore, the AE technique in conjunction with the k-means genetic algorithm provided a classification

of damage mechanisms under flexural load. The AE hits dominance results suggested that by strengthening the core with as low as 0.1 wt.% nanomaterials, core damage and fiber breakage can be minimized.

Regarding our preliminary studies and the previous work [11] related to the dispersion quality of CNT/CNC in distilled water, the underlying reasons of the poorer quality of specimens in which CNT and CNC had been used together, were considered to be related to drying process utilized in this study. Achieving even-sized nanoparticles and the repeatability of the process are two important issues need resolving in the oven drying and grounding methods employed in this study. Therefore, freeze-drying will be used as a reliable alternative method to preserve nano size of the particles as a next step of the work. Thus, with the removal of distilled water from the CNT/CNC/distilled water dispersion by sublimation, a more repeatable and reliable drying process will be achieved. Moreover, studies will be elaborated to find the optimum CNT/CNC amount for superior nano-reinforced foam-cored sandwich composites with retarded damage mechanisms.

Acknowledgment

This study was partially funded by the Scientific and Technological Research Council of Turkey (TUBITAK) Career Development Program 3501 (Project No. 121M993). The authors are also thankful to Mrs. Sakineh Fotouhi for the fruitful discussion on AE data processing, and Mr. İdris Gürkan for the advice about composite manufacturing processes.

References

[1] Ciecierska, E., Jurczyk-Kowalska, M., Bazarnik, P., Gloc, M., Kulesza, M., Kowalski, M., Krauze, S., and Lewandowska, M. “Flammability, Mechanical Properties and Structure of Rigid Polyurethane Foams with Different Types of Carbon Reinforcing Materials.” *Composite Structures*, Vol. 140, 2016, pp. 67–76. https://doi.org/10.1016/J.COMPSTRUCT.2015.12.022.

[2] Navidfar, A., Sancak, A., Yildirim, K. B., and Trabzon, L. “A Study on Polyurethane Hybrid Nanocomposite Foams Reinforced with Multiwalled Carbon Nanotubes and Silica Nanoparticles”, Polymer-Plastics Technology and Engineering, 2018, 57:14, 1463-1473, DOI: 10.1080/03602559.2017.1410834.

[3] Mahfuz, H., Zainuddin, S., and Jeelani, S. “Enhancing Fatigue Performance of Sandwich Composites with Nanophased Core.” *Journal of Nanomaterials*, Vol. 2010, 2010. https://doi.org/10.1155/2010/712731.

[4] Saha, M. C., Kabir, M. E., and Jeelani, S. “Enhancement in Thermal and Mechanical Properties of Polyurethane Foam Infused with Nanoparticles.” *Materials Science and Engineering: A*, Vol. 479, Nos. 1–2, 2008, pp. 213–222. https://doi.org/10.1016/J.MSEA.2007.06.060.

[5] Khan, T., Aydın, O. A., Acar, V., Aydın, M. R., Hülagü, B., Bayrakçeken, H., Seydibeyoğlu, M. Ö., and Akbulut, H. “Experimental Investigation of Mechanical and Modal Properties of Al2O3 Nanoparticle Reinforced Polyurethane Core Sandwich Structures.” *Materials Today Communications*, Vol. 24, 2020, p. 101233. https://doi.org/10.1016/J.MTCOMM.2020.101233.

[6] Septevani, A. A., Evans, D. A. C., Annamalai, P. K., and Martin, D. J. “The Use of Cellulose Nanocrystals to Enhance the Thermal Insulation Properties and Sustainability of Rigid Polyurethane Foam.” *Industrial Crops and Products*, Vol. 107, 2017, pp. 114–121. https://doi.org/10.1016/J.INDCROP.2017.05.039.

[7] Şerban, D. A., Weissenborn, O., Geller, S., Marşavina, L., and Gude, M. “Evaluation of the Mechanical and Morphological Properties of Long Fibre Reinforced Polyurethane Rigid Foams.” *Polymer Testing*, Vol. 49, 2016, pp. 121–127. https://doi.org/10.1016/J.POLYMERTESTING.2015.11.007.

[8] Yu, Y. H., Choi, I., Nam, S., and Lee, D. G. “Cryogenic Characteristics of Chopped Glass Fiber Reinforced Polyurethane Foam.” *Composite Structures*, Vol. 107, 2014, pp. 476–481. https://doi.org/10.1016/J.COMPSTRUCT.2013.08.017.

[9] Kim, M. S., Kim, J. D., Kim, J. H., and Lee, J. M. “Mechanical Performance Degradation of Glass Fiber-Reinforced Polyurethane Foam Subjected to Repetitive Low-Energy Impact.” *International Journal of Mechanical Sciences*, Vol. 194, 2021, p. 106188. https://doi.org/10.1016/J.IJMECSCI.2020.106188.

[10] Duc, H. M., Huu, D. N., Huu, T. T., Trong, L. le, Nhu, H. L., Ngoc, H. P., Van, T. N., Kieu Thi, Q. H., and Vu, G. N. “The Effect of Multiwalled Carbon Nanotubes on the Thermal Conductivity and Cellular Size of Polyurethane Foam.” *Advances in Polymer Technology*, Vol. 2021, 2021. https://doi.org/10.1155/2021/6634545.

[11] Ibanez Labiano, I., Arslan, D., Ozden Yenigun, E., Asadi, A., Cebeci, H., and Alomainy, A. “Screen Printing Carbon Nanotubes Textiles Antennas for Smart Wearables.” *Sensors 2021, Vol. 21, Page 4934*, Vol. 21, No. 14, 2021, p. 4934. https://doi.org/10.3390/S21144934.

[12] Assarar, M., Bentahar, M., el Mahi, A., and el Guerjouma, R. “Monitoring of Damage Mechanisms in Sandwich Composite Materials Using Acoustic Emission:” *http://dx.doi.org/10.1177/1056789514553134*, Vol. 24, No. 6, 2014, pp. 787–804. https://doi.org/10.1177/1056789514553134.

[13] Yang, R., He, Y., and Zhang, H. “Progress and Trends in Nondestructive Testing and Evaluation for Wind Turbine Composite Blade.” *Renewable and Sustainable Energy Reviews*, Vol. 60, 2016, pp. 1225–1250. https://doi.org/10.1016/J.RSER.2016.02.026.

[14] Masmoudi, S., el Mahi, A., and el Guerjouma, R. “Mechanical Behaviour and Health Monitoring by Acoustic Emission of Sandwich Composite Integrated by Piezoelectric Implant.” *Composites Part B: Engineering*, Vol. 67, 2014, pp. 76–83. https://doi.org/10.1016/J.COMPOSITESB.2014.05.032.

[15] Fotouhi, M., Sadeghi, S., Jalalvand, M., and Ahmadi, M. “Analysis of the Damage Mechanisms in Mixed-Mode Delamination of Laminated Composites Using Acoustic Emission Data Clustering:” *http://dx.doi.org/10.1177/0892705715598362*, Vol. 30, No. 3, 2015, pp. 318–340. https://doi.org/10.1177/0892705715598362.

[16] ben Ammar, I., Karra, C., el Mahi, A., el Guerjouma, R., and Haddar, M. “Mechanical Behavior and Acoustic Emission Technique for Detecting Damage in Sandwich Structures.” *Applied Acoustics*, Vol. 86, 2014, pp. 106–117. https://doi.org/10.1016/J.APACOUST.2014.04.016.

[17] Fotouhi, M., Saeedifar, M., Sadeghi, S., Najafabadi, M. A., and Minak, G. “Investigation of the Damage Mechanisms for Mode I Delamination Growth in Foam Core Sandwich Composites Using Acoustic Emission:” Vol. 14, No. 3, 2015, pp. 265–280. https://doi.org/10.1177/1475921714568403.

[18] Ji, X. long, Zhou, W., Sun, H., Liu, J., and Ma, L. hua. “Damage Evolution Behavior of Bi-Adhesive Repaired Composites under Bending Load by Acoustic Emission and Micro-CT.” *Composite Structures*, Vol. 279, 2022, p. 114742. https://doi.org/10.1016/J.COMPSTRUCT.2021.114742.

[19] Pashmforoush, F., Khamedi, R., Fotouhi, M., Hajikhani, M., and Ahmadi, M. “Damage Classification of Sandwich Composites Using Acoustic Emission Technique and K-Means Genetic Algorithm.” *Journal of Nondestructive Evaluation 2014 33:4*, Vol. 33, No. 4, 2014, pp. 481–492. https://doi.org/10.1007/S10921-014-0243-Y.

[20] Caglayan, C., Gurkan, I., Gungor, S., and Cebeci, H. “The effect of CNT-reinforced polyurethane foam cores to flexural properties of sandwich composites.” *Composites Part A: Applied Science and Manufacturing*, 115, 2018, 187-195.

[21] Kucukkalfa, E., Dincer, M., Karci, E., Vural, M. A., Yildiz, K., Ozden-Yenigun, E., Ozkendirici, B., and Cebeci, H. “Flexural Behaviour of Polyurethane Foam Filled High Performance 3-D Woven I-Beam Composites.” 20th European Conference on Composite Materials. Lausanne, Switzerland, 2022.

[22] Chen, L., Rende, D., Schadler, L. S., & Ozisik, R. “Polymer nanocomposite foams. Journal of Materials Chemistry A, 1(12), 3837-3850, 2013.

[23] Quispitupa, A., Shafiq, B., Just, F., and Serrano, D. “Acoustic Emission Based Tensile Characteristics of Sandwich Composites.” *Composites Part B: Engineering*, Vol. 35, Nos. 6–8, 2004, pp. 563–571. https://doi.org/10.1016/j.compositesb.2003.11.012.

[24] Emami Tabrizi, I., Oz, F. E., Seyyed Monfared Zanjani, J., Mandal, S. K., and Yildiz, M. “Failure sequence determination in sandwich structures using concurrent acoustic emission monitoring and postmortem thermography,” Mechanics of Materials, vol. 164, 2022, p. 104113.

[25] Oz, F. E., Ersoy, N., & Lomov, S. V. (2017). Do high frequency acoustic emission events always represent fibre failure in CFRP laminates?. Composites Part A: Applied Science and Manufacturing, 103, 230-235.